An Integrated Tactile and Thermal Sensor

David Siegel
Iñaki Garabieta
John M. Hollerbach

Massachusetts Institute of Technology Artificial Intelligence Laboratory
545 Technology Square
Cambridge, MA 02139

Abstract

The design, construction, and performance of a tactile sensor and a thermal sensor that can be combine into one compact device with both modalities is discussed. The tactile sensing portion is composed of an 8×8 array of force sensing cells with 1.8 mm center to center spacing. Heat transduction is measured by a 4×4 array of temperature sensors. A number of these devices will be mounted on the Utah-MIT four-fingered dextrous hand, providing a unique research environment for pursuing sensor driven control strategies.

Introduction

This paper examines the design, construction, and performance of a tactile sensor and thermal sensor for use with Utah-MIT dextrous hand [Jacobsen, et al. 1984]. The tactile portion is based on variations in the distance between two parallel plates of a capacitor [Siegel, Garabieta, and Hollerbach 1985; Boie 1984]. As force on a sensor point is increased, the gap between the plates of a capacitor will decrease. The measured capacitance is related to the distance between the plates, and hence the force being applied at that point. An 8×8 array of capacitor cells is utilized, giving the device 64 force sensitive tactile points. The thermal sensor [Siegel and Simmons 1985] measures heat conduction by heating an object, and measuring the resulting temperature change at the sensor's surface using a 4×4 array of surface mounted thermistors. The greater a material's thermal conductivity, the more rapidly the sensor's surface temperature will decline.

The sensor design process is complicated by the Utah-MIT hand's finger geometry. Most contact sensing technologies are unsuitable because fingertip space is limited and the sensors must be mounted on curved surfaces. Reliability is also of concern since the hand will be equipped with approximately a dozen sensors. Much effort was required to isolate durable materials and to find the construction and packaging techniques that satisfy these requirements, and give adequate sensing performance. More specifically, the design criterion for this project include:

- An 8×8 array with under 2 mm cell center to center spacing.
- A 4×4 array of thermal sensing cells mounted below the tactile transducers.
- A sensing technology that permits mounting the device on the non-planer surfaces of the hand.
- Low profile packaging; space at the finger mounting sites is at a premium.
- Space requirements for the wiring and electronics needed at the fingertips should be minimal.
- A compliant surface covering for increased prehension stability [Fearing and Hollerbach 1983].

This report describes the current state of this project, and the future directions of research that will be pursued with the sensor equipped dextrous hand.

This report describes research done at the Artificial Intelligence Laboratory of the Massachusetts Institute of Technology. Support for the laboratory's artificial intelligence research is provided in part by the System Development Foundation, in part by the Office of Naval Research under contract N00014-81-0494, and in part by the Advanced Research Project Agency under Office of Naval Research contracts N00014-80-C-050 and N00014-82-K-0334. Support for David M. Siegel is provided in part by a National Science Foundation fellowship, and for John M. Hollerbach in part by an NSF Presidential Young Investigator Award.

Contact Sensor Based Control

The use of contact sensor equipped dextrous hands in place of current robotic end-effectors will allow detailed study of the grasping and the manipulation of objects. For example, one of the many open questions in hand control is how to determine the most effective grasp orientation for a particular object geometry. The definition of "most effective" depends on the particular operation intended; for some tasks a power grip that imparts maximum holding force onto an object is best. Other times, a grip that gives an object its greatest mobility would be preferred.

Grasping operations are more complicated without knowledge of the contact point between the hand's fingers and an object. One important use for this information is to verify a grip's stability. If a grip is failing, contact sensors can provide information on the direction the object is slipping, possibly allowing corrective action to be taken. If the contact angle between a finger and an object is approaching the limits of the contact fictional cone, indicating that an unstable situation may be present, the finger orientations can be modified.

Delicate operations also require sensory feedback. To avoid breaking an egg, for example, the finger's contact force must be small, yet large enough to avoid slippage. Programming a hand to write on paper probably requires carefully monitoring the position of the pen with respect to the fingers and paper. Flipping the pages of a book is tricky as well; a light grip on the paper is required to avoid ripping the page, while enough contact force must be applied to generate the friction needed to flip the sheet upward. These operations are even hard for humans, as we all know from experience.[1]

A hand can be used for more than grasping and manipulating objects. Haptics, where the hand is used as an exploratory tool, is another important application. Exploratory motion is highly sensory driven; both contact sensors and joint positions provide information about an object and its environment. Texture and thermal clues can help a robot identify a material. Tracking an edge or seam to ascertain an object's outline can be done with tactile feedback. Detecting the orientation of a small part using its force contact profile is possible. Identifying a grasped object by mapping the finger contact locations to a library model has already been theoretically studied by Grimson and Lozano-Perez [1985].

[1] Humans, of course, learn from their mistakes. Ideally, a hand should also benefit from its failures. Contact sensors can also provide important information for automatically diagnosing why the planned operation failed, and what future corrective action would be best to take.

Assembly robots will benefit from the use of contact sensor equipped dextrous manipulators. Special purpose parts feeder might be replaced by a more general purpose hand. Contact sensors could resolve a part's location and orientation, allowing the assembly operation to proceed smoothly. Thermal sensors could assist in selecting a particular object from a bin of parts. For insertion operations the tactile system could detect jams, and then direct the hand to take the appropriate corrective action. A robot polishing the surface of a material could use texture detection to judge the quality of the finish.

It should be noted that machine vision can provide some, but not all, of the functionality of a contact sensing device. Thermal properties other than an object's temperature can only be obtained by a contact sensor. While vision can give useful views of an object provided adequate lighting is available, a contact sensor can provide some of the same information in the dark. An object's surface profile and texture can only be indirectly obtained from vision, with variations in lighting conditions and viewing angles effecting the results. Clearly, a contact force sensor obtains this information more accurately.

Fusion of data from multiple sensor sources supplemented by a knowledge base describing world objects will ultimately be possible. Using information contributed by different sensing modalities reduces the chance of error, increasing the robustness of the overall system. Humans are a good example of an integrated and intelligent sensor system. We receive information from touch, sound, sight, and smell. The brain uses clues extracted from these sources, along with general knowledge of our world, to make all its sensor related decisions.

Review of Sensor Technologies

Numerous contact sensors have been developed, employing a wide variety of transduction principles [Dario 1985]. Unfortunately, these sensors all fail to satisfy the previously stated requirements for use with the Utah-MIT hand. The most common shortcomings are in size, cell spacing, and ease of fabrication.

A wide variety of tactile sensor technologies have been reported in the literature. Conductive elastomers [Purbrick 1981; Overton and Williams 1981; Hillis 1982] deduce applied pressure from changes in resistance. These devices often suffer from low sensitivity and high hysteresis. Ferroelectric polymers [Dario, et al. 1984] have both thermal and pressure capabilites, but unfortunately lack static response. Optical devices [Jaconsen, et al. 1984; Begej 1984] are bulky, and often require large devices to scan the tactile cell array.

VLSI designs show perhaps the greatest promise for future tactile and thermal sensing device [Raibert and Tanner 1982; Raibert 1984; Chun and Wise 1985; Wong and Van der Spiegel 1985; Petersen 1985]. Today's designs, however, are plagued by reliablity and packaging difficulties. In essence, the greatest challanges to a sucessful VLSI sensor lie in the packaging domain, and not in the transduction processes themselves [Senturia and Day 1985].

Design Issues

This section describes the tactile sensor and the thermal sensor in detail. As previously mentioned, the devices are explicitly designed to be merged into one sensor incorporating both tactile and thermal capabilities. To be able to achieve this goal, the devices are to be stacked upon each other with the tactile sensor layered above the thermal sensor. The transduction processes selected and fabrication techniques employed make this possible.

Thermal Device

This sensor relies on the thermodynamic principle that heat will flow from a warmer material into a cooler material until their temperatures equalizes. The instantaneous rate of temperature change is related to the temperature differential between the materials, and their thermal conductivity properties.

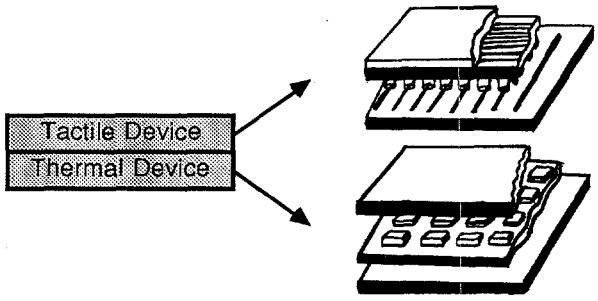

Figure 1: *Contact Sensor Design. Left: cross section of sensor. Right: exploded views of the tactile (upper) and thermal (lower) devices*

To measure thermal conductivity, the sensor applies heat to a material, and measures the rate of temperature change at its surface. The cooling rate is proportional to the material's thermal conductivity; a good heat conductor will rapidly reduce the sensor's temperature, while a better insulator will have the opposite effect.

More formally, a material's thermal properties can be characterized by its conductance and diffusivity. The coefficient of conductance, K, relates a temperature differential to a heat flow, according to

$$-K\frac{\partial v}{\partial x}. \tag{1}$$

This equation captures the intuitive notion that some materials conduct heat better than others; a high conductance lowers the temperature difference required for a particular heat flow.

A material's diffusivity is defined to be

$$\alpha = \frac{K}{\rho c}, \tag{2}$$

where K is its conductance, ρ is its density, and c is its specific heat. This parameter is related to the change in temperature of a unit volume as a unit temperature difference allows heat to flow into the object over a unit time interval. An inspection of the units of α will confirm this. The wide variety in common substances's conductivity and diffusivity insures different sensor response for different materials, and hence allows unique identification [Carslaw and Jaeger 1948].

To better understand the performance of the thermal sensor, a theoretical analysis of its behavior is presented. A simplified model of the sensor and the material being sensed that captures the essential parameters that effect the system's response is used. Fortunately, this model works well; the actual output of the sensor closely corresponds to the results obtained in this section.

The sensor can be modeled as a block at temperature $v(t)$ in contact with a material represented by an infinite rod at temperature $u(x,t)$. We are interested in finding the temperature at the contact point $x = 0$, where $u(0,t) = v(t)$, which represents the temperature of the sensor's thermistors. The material in this section is developed from the excellent discussion of heat conduction problems in Carslaw [1948].

The long rod's temperature $v(x,t)$, in one dimension, is given by the diffusion equation

$$\frac{\partial^2 v}{\partial x^2} - \frac{1}{\alpha}\frac{\partial v}{\partial t} = 0, \tag{3}$$

where α is the material's thermal diffusivity.

The boundary condition for equation 3, which describes the interface between the block and the rod, is given by

$$Mc\frac{du}{dt} - K\frac{\partial v}{\partial x} = Q, \tag{4}$$

where $u(t)$ is the sensor's temperature, M is the sensor's mass, c is the sensor's specific heat, Q is the sensor's heat output, and K is the sensed material's thermal conductivity. Intuitively, this equation indicates that some of the heat the sensor produces is absorbed by the sensor itself, while the rest flows into the material being sensed. Since the rod is assumed to be infinite in length, this is the only boundary condition required.

We now must find a solution for $v(x,t)$ which satisfies boundary condition 4 and the governing equation 3. Using the Laplace transform we obtain:

$$v(x,t) = \frac{2Q}{K}\sqrt{\frac{\alpha t}{\pi}}e^{\frac{-x^2}{4\alpha t}} - \frac{Q(1+hx)}{Kh}\mathrm{erfc}(\frac{x}{2\sqrt{\alpha t}}) + \frac{Q}{Kh}e^{hx+h^2\alpha t}\mathrm{erfc}(\frac{x}{2\sqrt{\alpha t}} + h\sqrt{\alpha t}) + V_0 e^{hx+h^2\alpha t}\mathrm{erfc}(\frac{x}{2\sqrt{\alpha t}} + h\sqrt{\alpha t}), \quad (5)$$

where

$$h = \frac{K}{Mc\alpha},$$

and where *erfc* is the Gaussian error function,

$$\mathrm{erfc}(x) = 1 - \frac{2}{\sqrt{\pi}}\int_0^x e^{-\phi^2}d\phi. \quad (6)$$

From equation 5 we obtain the general behavior of the sensor as contact with a material is made. Since the *erfc* function approaches zero rapidly, the initial output will fall from V_0 to

$$\frac{2Q}{K}\sqrt{\frac{\alpha t}{\pi}} - \frac{Q}{Kh}. \quad (7)$$

Increasing the sensor's mass M reduces both speed and sensitivity. Increasing the heat output Q has little effect on the initial temperature falloff, but ultimately increases the measured surface temperature. An examination of plots of theoretical output for different levels of thermal diffusivity and conductivity indicate that positive material classification can be made in under one second. It is useful to keep these results in mind as we next discuss the sensor's fabrication.

The thermal transducers will form the lower layer of the overall device, as shown in Figure 1. A 4×4 matrix of surface mounted thermistors are placed on a 1.0 mm thick flexible printed circuit board (FPCB). To provide protection and a smooth surface covering, a layer of heat conducting silicone rubber is molded over the top surface of the array, and in the gaps between the thermistors themselves. A thin electrical insulator covers the back traces of the FPCB. Heat is generated by applying a current through conductive paint applied onto the insulating covering.

To minimize the number of interconnection wires that are needed to scan the array, matrix scanning with analog multiplexing is employed. To read the value of a particular column of thermistors, a driving voltage is applied using the column multiplexor, while the other columns are tied to ground. The sensor's rows are connected to operational amplifiers with negative feedback. Hence, their outputs are proportional to the resistances of the selected column thermistors.

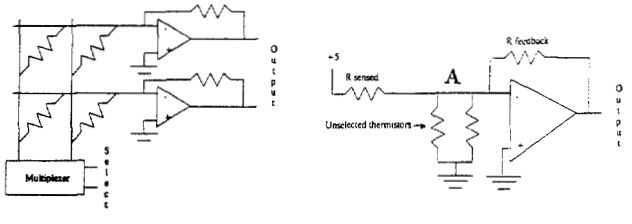

Figure 2: *Left: schematic of 2×2 array version of the thermal sensor. Right: effective schematic of sensor with one column selected.*

The schematic diagrams in Figure 2 show the the scanning electronics and the effective electrical circuit when one column of thermistors have been selected. Since node A is at a virtual ground, there will be no voltage difference across the unsensed thermistors, and no appreciable current will flow through them. Only the selected column thermistor will affect the amplifier's output. Hence, the resistance of the desired thermistor can be inferred from the voltage output of the amplifier.

Tactile Device

A capacitive based tactile sensor measures an applied force by detecting changes in the distance between two parallel plates of a small capacitor. As force is increased, the dielectric material between the plates will compress, increasing their effective capacitance. Using simple electronics, the variation in capacitance is measured, and then converted to a voltage output proportional to the applied force.

An array of capacitive cells is formed by sandwitching a dielectric layer between two sets of parallel conducting traces, with the top etches perpendicular to the bottom ones, hence forming a capacitor at each of their intersections. This structure is to be mounted above the thermal layer, and to be placed in firm contact with the heat conductive silicone rubber protecting the thermistors. Figure 1 outlines the design of an 8 × 8 array with 64 force sensing cells.

The dielectric material is one of the most important sensor components. It serves the dual purpose of translating force into positional changes, and forming the dielectric gap between the capacitive plates. Ideally, it should compress linearly as force on it increases. This behavior, found in a spring and described by Hooke's law, is given by:

$$F = k\Delta X, \quad (8)$$

where F is the applied force, k is the effective spring constant, and ΔX is the positional change that the force produces. Having a material that closely approximates this equation makes it easy to translate the output of the sensor back to applied force.

The dielectric layer is composed of thermally conductive silicone rubber. Since the tactile array is to be mounted above the thermal array, this material permits heat to flow more freely between the dielectric and the surface of the sensor. In addition, silicone rubber has desirable flexibility, and can be formed into appropriate shapes using injection molding. A solid sheet of rubber, however, does not compress desirably. Since silicone rubber is largely incompressible, pushing down on it in one place will force the material up in another place. To overcome this problem, we have formed the material into a sheet with protruding round tabs. As pressure is applied to its top, the little tabs compress, and the material expands to fill the surrounding air gaps. As later experiments will show, the molded dielectric's positional response to an applied force is fairly linear.

The dielectric is constructed so each capacitor in the sensor array has a tab between it. The current dielectric has a 0.25 mm thick backing with the tabs protruding out from 0.25 mm to 0.75 mm, depending on the desired force range. The tab diameter is 1.4 mm.

The lower conducting rows are etched onto a two sided flexible printed circuit board. Small ground traces are routed between these conductors to reduce electrical cross-talk. The upper conducting columns are to be silk screened onto the top of the dielectric layer using a silver based conductive silicone rubber. The initial prototype tested within this paper, however, uses conducitve trace painted onto a thin sheet of mylar. Finally, the top of the sensor is covered with an electrically conductive material to shield the capacitive cells from external electrical fields.

To design the detection electronics, it is necessary to estimate the capacitance of a sensor cell. Hopefully, its magnitude will be large enough to permit detection with relatively simple electronics, keeping the size and cost of the sensor within reasonable limits. The capacitance of two parallel plates, in electrostatic

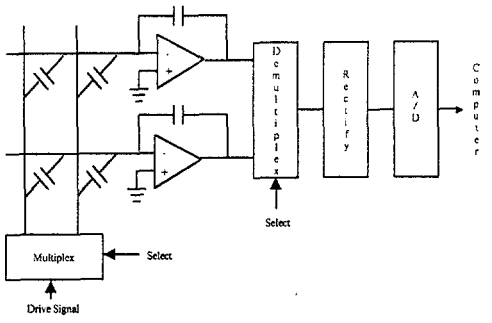

Figure 3: *Tactile scanning electronics schematic diagram.*

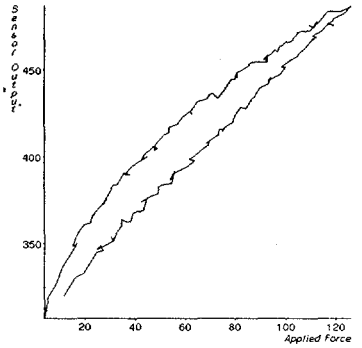

Figure 4: *Tactile sensor output verses applied force.*

units, is given by:

$$C = \frac{\alpha A}{4\pi d}, \tag{9}$$

where α is the dielectric constant of the separation material, and d and A are the separation distance and area of the two plates, respectively. If we assume $d = 0.025$ cm, $A = 0.16$ cm^2, a dielectric constant of 4 [Weast 1968], and that the farad $= 9 \times 10^{11}$ electrostatic units, the nominal capacitance for a force cell is approximately 0.2 pf. Experimentally, we have found that the value is closer to 0.5 pf, possibly due to a higher than expected dielectric constant. This value is large enough to detect if ample electrical shielding is provided to reduce external stray capacitance.

The sensor's scanning electronics are based on an amplitude modulation scheme. In essence, a cell is connected to the inverting input of an operational amplifier with a small capacitor in its feedback loop. A driving signal applied to the cell will modulate the amplifier's output according to the ratio given by:

$$V_{out} = -V_{in}\frac{C_{cell}}{C_{feedback}}. \tag{10}$$

If a driving signal is sequentially applied to each row, and the unselected rows are tied to ground, each column amplifier's output will correspond to the selected row's capacitance. Using this scheme, the capacitance of each cell in the array can be unambiguously obtained.

To provide the driving signal, a 200 kilohertz waveform is multiplexed into the rows. The column amplifier outputs are demultiplexer with an analog switch, rectified, amplified, and filtered before being converted to a digital signal for computer processing, as shown in Figure 3.

Since the amplifier's positive input is tied to ground, its negative input will be held at a virtual ground. This allows all the sensor columns to be held at the same potential of the ground planes enclosing the device, helping to minimize stray capacitance effects, and increasing overall sensitivity. In addition, this helps reduce cross capacitance between adjacent rows, since there is no voltage difference between them.

Experimental Results

In this section, the results of a series of experiments designed to quantify the sensor's performance are reviewed. The tactile sensor and the thermal sensor have been tested separately. We are now in the process of merging the two devices together, but performance results are not yet available.

A contact sensor test station has been used to conduct these experiments. The station uses a computer controlled positioning table to move the sensor array and has a computer controlled probe to apply a precise force at the selected location. The test station allows very accurate performance data to be gathered, and experiments can be conducted repeatidly to test for response variation over time.

Tactile Force Sensitivity

Using the test station, a force was applied to the sensor array using a round probe tip at a fixed location. The sensor response at that point is shown in Figure 4. The upper curve corresponds to the sensor output for an increasing applied force. The lower curve is for a decreasing force. The difference between the curves is the device's hysterisis, which is approximetaly 5 percent of total response.

The device's overall sensitivity was obtained by repeating the force test many times, and computing the standard deviation of the response. We found that a force in the 0-200 gram range can measured with 7 bits of accuracy.

As previously mentioned, the device's force sensitivity is a direct function of the compressibility of the elastic/dielectric layer. The achieved sensitivity was chosen out of convenience, not necessity; the selected range was felt to be most useful for our applications. It would be easy to construct a family of sensors that covered a variety of different force scales, should the need arise.

Tactile Spatial Resolution

The spatial resolution of the sensor is limited by the spacing between capacitive cell centers and the elastomeric properties of the dielectric and protective coverings. For a sensor that records just surface normal force, a point source should only be detected by the one or more cells directly in contact with the stimuli; spreading or blurring to adjacent cells should be minimal. Obviously, having a sharp sensor response will give more detail in tactile force outlines of probed objects. In some cases, however, it may be useful to propagate strains between adjacent sensor sites. Fearing and Hollerbach [1984] theoretically show how strain sensors placed below a surface can extract the angle of inclination, location, and magnitude of a load line.

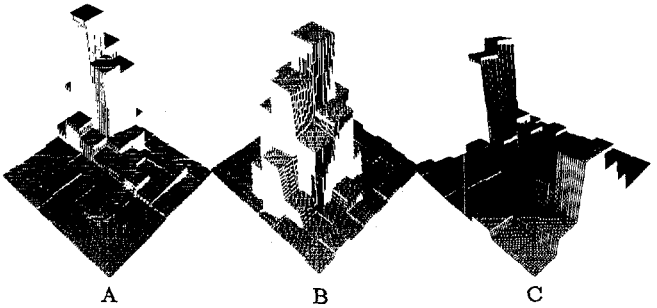

Figure 5: *Force response to blunt tipped probes, from left to right: small probe, large probe, two probes at each end of the pad.*

To determine the spatial resolution of our device, blunt tipped rods of varying diameters were pressed against the sensor pad, and the resulting force profiles were recorded. Bar plots *A* and *B* in Figure 5 show the sensor's output for two different sized probes. By observing the sharp cutoff in response at the edges of the force peaks, we can conclude that the blurring and crosstalk between adjacent sensor cells is very low. In both cases, the force peaks occur directly at the points of contact. Plot *C* shows the sensor output as two small probes are pressed at opposite ends of the pad. No crosstalk between the stimuli is present.

Tactile Shape Discrimination

The shape of an object can be obtained by pressing the tactile sensor against it, and recording the resultant force profile. In cases where visual inspection is impossible, such as when a manipulator end-effector obscures the view, this is especially desirable. The spatial resolution results of the previous section indicate that the sensor's shape discrimination ability should be good. To verify this, several small objects were pressed against the tactile pad, and the force outputs were recorded.

Figure 6 shows binary threshold versions of the sensor's output for these objects. We chose to display the response in this form to emphasize the outline of the objects, and to avoid some calibration issues. Since each force cell has a somewhat different though repeatable response, the array must first be normalized and calibrated to compare the output of all the cells together, in one force image.

Thermal Material Recognition

One of the primary applications for the thermal sensor is recognition of an unknown material from a library of thermal profiles. From the previous discussion we can expect that the temperature at the surface of the sensor will drop at an exponential rate when placed in contact with an object. The shape and final value of this curve is related to both the diffusivity and conductivity of the sensed object, in addition to characteristics of the sensor itself. Material recognition can be established by matching the sensor's response to a library of response curves, where a good match constitutes identification.

To measure recognition effectiveness, wood, nylon, and steel were placed in contact with the sensor, and the temperature over time response was recorded. Figure 7 shows the response of one pixel in the sensor array as contact with the materials is made. The large difference in sensor output for each of these materials would make recognition readily possible.

It should be noted that the surface texture of a material being sensed affects its overall thermal profile. This result is caused by variations in the quality of the thermal contact made between the sensor and the sensed object. A rough texture has many gaps in its surface. The gaps are filled with air, and form a thermal insulation layer between the sensor and the object. Since material identification is made by comparing a thermal response

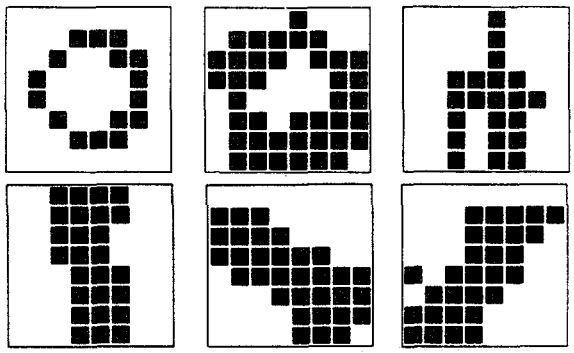

Figure 6: *Thresholded sensor output. First row: two washers and an electrical connector lug. Second row: three rectangular blocks pressed at different angles.*

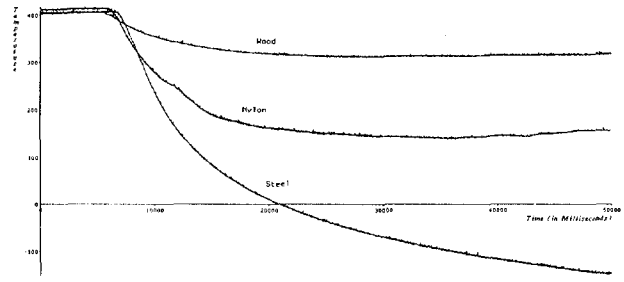

Figure 7: *Sensor response for wood, nylon, and steel.*

curve with a library of such curves, this effect should not cause problems with recognition. In fact, the ability to distinguish surface textures can be an advantage in some situations.

Thermal Temperature Recovery

After the sensor is cooled by making contact with a material, some time is required for return to its steady state temperature. To measure this recovery period a block of aluminum was placed on the sensor and then removed. A rather long 18 seconds elapsed for a 90 percent recovery, as shown in Figure 8. This period could be reduced by increasing the heat output of the device. However, reusing the sensor before it reaches its steady state temperature is also possible. The shape of the response curve is independent of the sensor's starting temperature, as long as a reasonable temperature differential initially exists.

Thermal Spatial Sensitivity

The 4×4 thermistor array gives "thermal conduction images" of objects. This information can be used to determine a material's position on the grid, in addition to its heat conduction properties. The plots in Figure 9 show the array's response to an aluminum rod alone, and an aluminum and wooden rod together, where the height of a cell is proportional to the thermal conductivity measurement at that point.

Discussion

The sensors described within this paper have both tactile and thermal capabilities, and are suitable for mounting on the fingers of the Utah-MIT dextrous hand. Special attention was given to the transduction methods employed and the fabrication processes utilized to ensure adequate performance and reliability. Ultimately the sensor equipped hand will be used for exploring haptic sensing and grasping strategies; the wealth of contact data this device provides makes it especially useful for these purposes.

Two of our initial design criterion were to ensure adequate reliability and repeatability over extended periods of use. The prototype sensors have now been in use for 6 months, and little or no performance degradation has been detected. The simplicity of the sensors is at least partially responsible for this sucsess.

The next stage of this project is to complete the fabrication of the combine tactile and thermal sensor, and to mount them onto

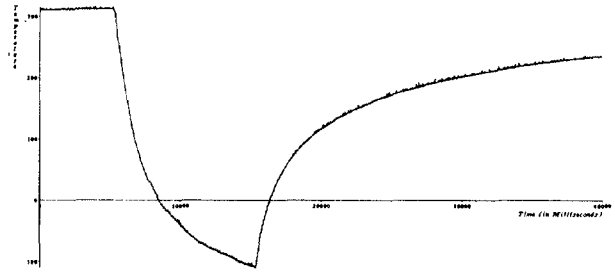

Figure 8: *Temperature recovery after an object is removed from the sensor.*

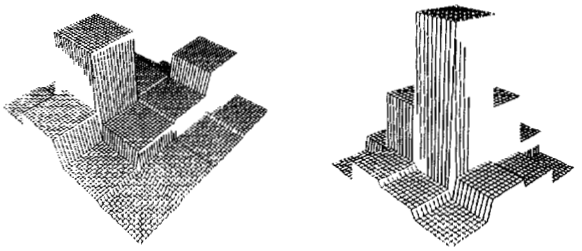

Figure 9: *Thermal array responses. Right: aluminum rod. Left: aluminum and wooden rod.*

several surfaces of the Utah-MIT hand. We hope to accomplish this within the next several months. With this, we will be a small step closer to our goal of duplicating the perception capabilities of the human finger, ultimately giving us a better understanding of our biological sensory and motor control systems.

Acknowledgments

Discussions with various members of the MIT Artificial Intelligence Laboratory have been helpful throughout this project. In particular, Scott Jones, Sundar Narasimhan, and Laurel Simmons have provided valuable assistance. The graphs in this report were made possible by Harry Voorhees' elegant plotting package.

References

S. Begej, "An Optical Tactile Array Sensor," *SPIE Conference on Intelligent Robots and Computer Vision,* pp. 271-280, Cambidge, MA, 1984.

R. A. Boie, "Capacitive Impedance Readout Tactile Image Sensor," *IEEE International Conference on Robotics,* pp. 370-378, Atlanta, March 1984.

H. S. Carslaw, J. C. Jaeger, "Conduction of Heat in Solids," Oxford at the Clarendon Press, Great Britain, 1948.

Chomerics, "EMI Shielding Engineering Handbook," Woburn, MA, 1985.

K. J. Chun, K. D. Wise, "A Capacitive Silicon Tactile Imaging Array," *IEEE International Conference on Solid-State Sensors and Actuators,* pp. 22-25, Philadelphia, PA, June 1985.

P. Dario, D. De Rossi, C. Domenici, R. Francesconi, "Ferroelectric Polymer Tactile Sensors with Anthropomorphic Features," *IEEE International Conference on Robotics,* pp. 332-340, Atlanta, GA, March 1984.

P. Dario, D. De Rossi, "Tactile Sensors and the Gripping Challenge," *IEEE Spectrum,* Vol. 22, No. 8, August 1985.

R. S. Fearing, J. M. Hollerbach, "Basic Solid Mechanics for Tactile Sensing," *IEEE International Conference on Robotics,* pp. 266-275, Atlanta, GA, March 1984.

W. E. L. Grimson, T. Lozano-Perez, "Model Based Recognition and Localization from Tactile Data," *IEEE International Conference on Robotics and Automation,* St. Louis, 1985.

W. D. Hillis, "A High-Resolution Imaging Touch Sensor," *The International Journal of Robotics Research,* Vol. 1, No. 2, pp. 33-44, 1982.

S. C. Jacobsen, J. E. Wood, D. F. Knutti, K. B. Biggers, "The Utah-MIT Dextrous Hand: Work in Progress," *The International Journal of Robotics Research,* Vol. 3, No. 4, pp. 21-50, 1984.

K. J. Overton, T. Williams, "Tactile Sensation for Robots," *7th International Joint Conference on Artificial Intelligence,* Vancouver, Canada, Aug. 1981.

K. Petersen, C. Kowalski, J. Brown, "A force Sensing Chip Designed for Robotic and Manufacturing Automation Applications," *IEEE International Conference on Solid-State Sensors and Actuators,* pp. 30-32, Philadelphia, PA, June 1985.

J. A. Purbrick, "A Force Transducer Employing Conductive Silicone Rubber," *Proceedings of the 1st International Conference on Robot Vision and Sensory Controls,* pp. 73-80, Stratford-upon-Avon, UK, April 1981.

M. H. Raibert, J. E. Tanner, "Design and Implementation of a VLSI Tactile Sensing Computer," *The International Journal of Robotics Research,* Vol. 1, No. 3, pp. 3-18, 1982.

M. H. Raibert, "An All Digital VLSI Tactile Array Sensor," *IEEE International Conference on Robotics,* pp. 314-319, Atlanta, GA, March 1984.

S. D. Senturia, D. R. Day, "An Approach to Chemical Microsensor Packaging," *IEEE International Conference on Solid-State Sensors and Actuators,* pp. 198-201, Philadelphia, PA, June 1985.

D. M. Siegel, I. Garabieta, J. M. Hollerbach, "A Capacitive Based Tactile Sensor," *SPIE Conference on Intellegent Robots and Computer Vision,* Cambridge, MA, Sept. 1985.

D. M. Siegel, L. Simmons, "A Thermal Based Sensor System," *SME Sensors '85 Conference,* Detroit, MI, Nov. 1985.

R. C. Weast, Editor, "Handbook of Chemistry and Physics," The Chemical Rubber Co., Cleveland, OH, 1968.

K. Wong, J. Van der Spiegel, "A Shielded Piezoresistive Tactile Sensor Array," *IEEE International Conference on Solid-State Sensors and Actuators,* pp. 26-29, Philadelphia, PA, June 1985.